Fairing Triangular *B*-splines of Arbitrary Topology

Ying He, Xianfeng Gu, and Hong Qin
Stony Brook University
E-mail: {yhe|gu|qin}@cs.sunysb.edu

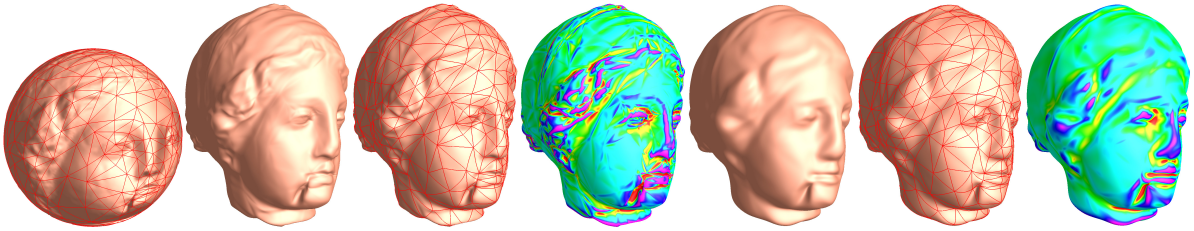

Figure 1. Fairing a spherical triangular *B*-spline. (a) shows the spherical domain with 682 triangles. (b), (c) and (d) show a degree 5 (C^4 continuous) spherical spline and its mean curvature plot. Note that the spline surface has high curvature concentration along the image of edges of the spherical triangles. (e), (f) and (g) show the spline generated by our automatic fairing method. The computational time is 8 seconds on a 3GHz Pentium IV PC. Compared to the surface in (b), the shape of the smooth spline (e) does not change too much, but the curvature distribution improves significantly. The red curves in (c) and (f) correspond to the edges in the spherical triangulation.

Abstract

Triangular B-splines are powerful and flexible in modeling a broader class of geometric objects defined over arbitrary, non-rectangular domains. Despite their great potential and advantages in theory, practical techniques and computational tools with triangular B-splines are less-developed. This is mainly because users have to handle a large number of irregularly distributed control points over arbitrary triangulation. In this paper, we propose an automatic and efficient method to generate visually pleasing, high-quality triangular B-splines of arbitrary topology for shape fairing. Our experimental results on several real datasets show that triangular B-splines are powerful and effective in both theory and practice.

Keywords: Triangular *B*-splines, fairing algorithm.

1. Introduction

Triangular *B*-splines, introduced by Dahmen, Micchelli, and Seidel [1], are emerging as a novel and powerful tool for shape modeling because they can represent, without any degeneracy, complex geometric surfaces defined on open and irregular parametric domains. Triangular *B*-splines are even more powerful when being extended and generalized to spherical domain [5] and manifold of arbitrary topology [3]. Therefore, triangular *B*-splines can potentially serve as a geometric standard for product data representation and model conversion in shape design and processing.

Despite their aforementioned geometric advantages and modeling potential over popular tensor-product splines, triangular *B*-splines have not been widely used in research community and CAD industry. This is mainly because 1) users must deal with a large number of irregularly-distributed control points to make certain non-intuitive decisions on their placements; 2) triangular *B*-splines have the so-called knot line, where the surface curvature distribution along the curved triangular boundaries (corresponding to the edges in the domain triangulation) is much worse than other regions, and there exist no effective approaches to control the overall curvature distribution and improve the shape quality via automatic control-point adjustment.

All the existing literatures of triangular *B*-splines focus on either theoretical foundation or evaluation/data fitting algorithms. No previous work has been done in the surface quality analysis of triangular *B*-splines. This paper aims at providing such tools to generate visually pleasing triangular *B*-splines without the need of any tedious manual operation on control points. Our method solves a simple least square with linear constraints. Therefore, our approach is both fast and robust. Furthermore, this new method works for planar, spherical, and manifold triangular *B*-splines without any theoretical difficulties.

2. Fairing Triangular *B*-splines

2.1. Construction of triangular *B*-splines

The planar triangular *B*-spline is proposed by Dahmen, Micchelli and Seidel in [1]. Pfeifle and Seidel successfully generalize the planar triangular B-splines to the spherical domain [5]. Recently, Gu, He and Qin [3] systematically build the theoretic framework of manifold

spline, which locally is a traditional planar spline, but globally defined on the manifold.

The constructions of planar and spherical triangular *B*-splines are simple and straightforward. In the interests of space, we only briefly introduce the construction of manifold triangular *B*-spline: Given a triangular mesh of arbitrary topology with or without boundaries, we first compute the global conformal parameterization of the domain manifold [4]. Then, we compute a special atlas covering the manifold, such that the transition functions are affine. Next, we define the sub-knots on the manifold directly. Finally, we define basis functions on the chart and assign control point to each basis function.

The planar, spherical and manifold triangular B-splines can be written in the same fashion:

$$\mathbf{F}(\mathbf{u}) = \sum_I \sum_{|\beta|=n} \mathbf{c}_{I,\beta} N(\mathbf{u}|V_\beta^I), \quad \mathbf{u} \in M \tag{1}$$

where $\mathbf{c}_{I,\beta}$ is the control point and M is the domain.

Triangular *B*-splines have many valuable properties which are desirable for geometric modeling. For examples, triangular *B*-splines are piecewise polynomial defined on the parametric domain of arbitrary triangulation. Therefore, the computations of various differential properties are robust and efficient. The degree n triangular *B*-spline is of C^{n-1} continuous everywhere if there are no degenerate knots. Furthermore, by intentionally placing knots along the edges of the domain triangulation, we can model sharp features easily. The manifold spline of genus g has no more than $2g-2$ singular points while planar and spherical splines do not. Table 1 summarizes the properties of triangular *B*-splines for shape modeling.

2.2. Fairing algorithm

Fairing is of central importance during the design process of free form surfaces. Conventional methods for local and global fairing usually involve a physics based fairness criterion, e.g., membrane energy and thin-plate energy. Note that these fairness functionals involve the integration of the derivatives of $\mathbf{F}$ over the parametric domain. Calculating the exact value of the fairness functional is challenging for triangular *B*-splines, since there is no restriction on the domain triangulation and the sub-knots are also distributed irregularly. In this paper, we propose a new post-processing fairing method which does not need the computation of the complicated double integral. Instead, it only relies on a set of linear constraints of the control points.

Our method is inspired by the knot-line elimination work of Gormaz [2]. Although triangular *B*-spline has C^{n-1} continuity if there are no degenerate knots, the spline surfaces may not be smooth as one expected. The curvature along the images of the edges in the parametric domain is larger than other regions. Fig. 3 shows a degree 4 planar triangular B-spline, which is C^3 continuous everywhere. However, the surface is not visually smooth due to the high curvature concentration along the edges of adjacent spline patches. This phenomenon is called "knot line" of the triangular *B*-splines.

Given a degree n triangular *B*-spline surface $\mathbf{F}(\mathbf{u})$ defined on arbitrary triangulation, consider two domain triangles $\Delta(I) = [\mathbf{t}_0^I, \mathbf{t}_1^I, \mathbf{t}_2^I]$ and $\Delta(J) = [\mathbf{t}_0^J, \mathbf{t}_1^J, \mathbf{t}_2^J]$ such that $\Delta(I)$ and $\Delta(J)$ are adjacent. For example, suppose $\mathbf{t}_0^I = \mathbf{t}_0^J$ and $\mathbf{t}_1^I = \mathbf{t}_1^J$ (see Fig. 2). Therefore, the sub-knots satisfy $\mathbf{t}_{0,i}^I = \mathbf{t}_{0,i}^J$ and $\mathbf{t}_{1,i}^I = \mathbf{t}_{1,i}^J$, for $i = 1,...,n$. Let $\mathbf{F}^I$ be the piecewise polynomial restricted on the triangle $\Delta(I)$, i.e., $\mathbf{F}^I(\mathbf{u}) = \sum_{|\beta|=n} \mathbf{c}_{I,\beta} N(\mathbf{u}|V_\beta^I)$. Let f^I be the polar form of $\mathbf{F}^I$. Similarly, we define $\mathbf{F}^J$ and f^J, respectively(see [6] for the details of polar form). Then, Gormaz proves [2]:

The spline surface $\mathbf{F}(\mathbf{u})$ *has no discontinuity of its n-th derivative along the lines*

$$[\mathbf{t}_{0,\beta_0}^I, \mathbf{t}_{1,\beta_1}^I], \forall \beta, \ |\beta| = n, \beta_2 \le r$$

$$\textit{iff} \ \ \mathbf{c}_{I,\beta} = f^J(V_\beta^I), \forall \beta, \ |\beta| = n, \beta_2 \le r \tag{2}$$

where $0 \le r \le n-1$, $V_\beta^I = \{t_{0,0}^I,...,t_{0,\beta_0-1}^I,...,t_{2,0}^I,...,t_{2,\beta_2-1}^I\}$.

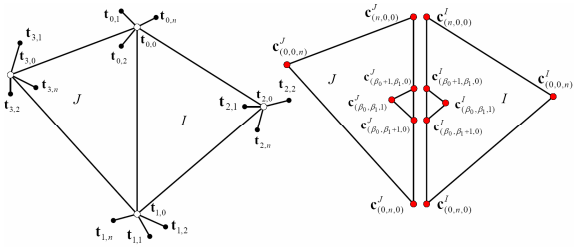

Figure 2. Illustration of Equation (2) for $r = 1$. *Left*, parametric domain; *Right*, control points.

Eq. (2) defines the affine relations between the control points of $\mathbf{F}^I(\mathbf{u})$ and $\mathbf{F}^J(\mathbf{u})$. Given a $r \in [0, n)$, let the control points satisfying Eq. (2), then the discontinuity along certain knot lines disappear, and the curvature distribution along those lines improves. Fig. 2 illustrates the case $r = 1$. For $\beta = (\beta_0, \beta_1, 1)$, Eq. (2) is written as

$$\mathbf{c}_{(\beta_0,\beta_1,1)}^I = \frac{d(\mathbf{t}_{2,0}, \mathbf{t}_{1,\beta_1}, \mathbf{t}_{3,0})}{d(\mathbf{t}_{0,\beta_0}, \mathbf{t}_{1,\beta_1}, \mathbf{t}_{3,0})} \mathbf{c}_{(\beta_0+1,\beta_1,0)}^J + \frac{d(\mathbf{t}_{0,\beta}, \mathbf{t}_{2,0}, \mathbf{t}_{3,0})}{d(\mathbf{t}_{0,\beta_0}, \mathbf{t}_{1,\beta_1}, \mathbf{t}_{3,0})} \mathbf{c}_{(\beta_0,\beta_1+1,0)}^J + \frac{d(\mathbf{t}_{0,\beta_0}, \mathbf{t}_{1,\beta_1}, \mathbf{t}_{2,0})}{d(\mathbf{t}_{0,\beta_0}, \mathbf{t}_{1,\beta_1}, \mathbf{t}_{3,0})} \mathbf{c}_{(\beta_0,\beta_1,1)}^J$$

where $d(\cdot,\cdot,\cdot)$ is the determinant function. It is easy to verify that Eq. (2) is just a linear combination of the

control points for $0 \le r \le n-1$.

In the following, we consider the global fairing problem of triangular *B*-splines. Given a (planar, spherical or manifold) triangular *B*- spline surface $\mathbf{F}(\mathbf{u})$, we want to find a faired surface $\widetilde{\mathbf{F}}(\mathbf{u})$ such that $\widetilde{\mathbf{F}}$ approximates the original surface $\mathbf{F}$ as much as possible. This leads to the following least square problem:

$$\min_{\widetilde{\mathbf{c}}} \sum_{I} \sum_{|\beta|=n} \left\| \widetilde{\mathbf{c}}_{I,\beta} - \mathbf{c}_{I,\beta} \right\|^2 \qquad (3)$$
$$\text{subject to } \widetilde{\mathbf{c}}_{I,\beta} = f^J(V_\beta^I), \forall I, \forall \beta, |\beta| = n, \beta_2 \le r$$

In the objective function, we minimize the squared distance between the control points of the original and the new spline surface, which implies that the minimal change of the shape. In the constraints, we use an integer $r \le n-1$ to control the fairness of the spline surface. The bigger value r, the more faired surface we obtain. In our experiments, we can get visually pleasing surfaces with $r = 1$ or $r = 2$.

As mentioned above, the constraints in Eq. (3) are just linear equations of the control points. Therefore, Eq. (3) is a linear constrained quadratic programming problem which has the following form:

$$\min_{x} \frac{1}{2} x^T I x + c^T x + f \qquad (4)$$
$$\text{subject to } Ax = b$$

where I is the identity matrix. In our implementation, we solve the above problem using Lagrange multipliers approach. Fig. 3 illustrates the fairing algorithm to a planar triangular *B*-spline.

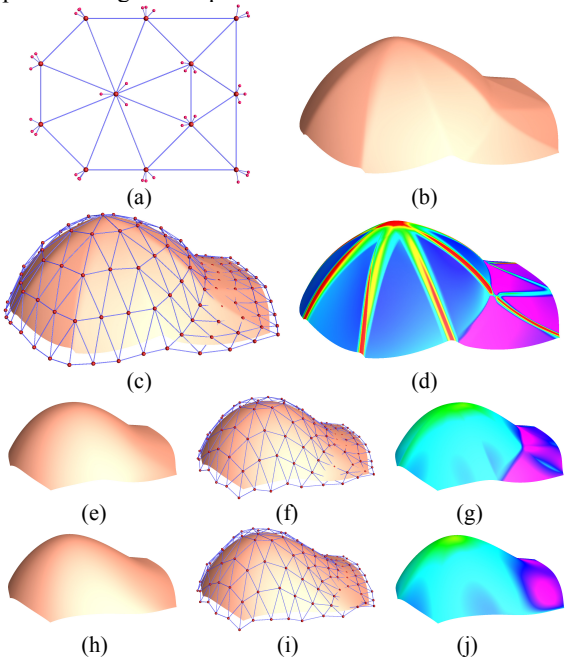

Figure 3. Illustration of our fairing algorithm to a degree 4 planar triangular *B*-spline: (a) shows the parametric domain. (b) and (c) show the spline surface and the control net respectively. (d) shows the mean curvature plot of the spline surface. Note that the curvature along the image of edges on the domain triangulation is significantly larger than the vicinity. (e), (f) and (g) show fairing the spline surface with $r = 1$. (h), (i) and (j) show fairing the spline surface with $r = 2$.

2.3. Experimental results

We have implemented a prototype system on a 3GHz Pentium IV PC with 1GB RAM. We perform experiments on several models ranging from planar triangular *B*-splines to manifold triangular *B*-splines. Table 2 shows the statistics of our test cases. As shown in Fig. 1, 3, and 4, we can obtain highly smooth triangular B-spline surfaces of various topological types.

Table 2. Statistics of test cases: n, degree of spline surface; N_t, # of domain triangles; N_c, # of control points; r, smoothness factor. The execution time measures in seconds.

Object	Type	n	N_t	N_c	r	Time
Cap	planar	4	13	123	2	<1s
Face	planar	5	251	3181	2	2s
Venus	spherical	5	682	8527	2	8s
Dog	spherical	5	656	8202	2	7s
Bottle	manifold	3	1889	8513	1	6s

3. Conclusion

In this paper, we have proposed an automatic and efficient method to generate visually pleasing, high-quality triangular *B*-splines of arbitrary topology for shape fairing and control. Our method is both fast and robust, as only a system of linear equations is solved. Our experimental results on several real datasets have demonstrated that triangular *B*-splines are powerful and effective in both theory and practice.

References

[1] W. Dahmen, C.A. Micchelli, and H.-P. Seidel, "Blossoming begets *B*-spline bases built better by *B*-patches", *Mathematics of Computation*, 59(199):97-115, 1992.

[2] R. Gormaz, "*B*-spline knot-line elimination and Bézier continuity conditions", In *Curves and Surfaces in Geometric Design,* pp. 209-216, A.K. Peters, 1994.

[3] X. Gu, Y. He, and H. Qin, "Manifold splines", In *Proceedings of ACM SPM '05,* pp.27-38, 2005.

[4] X. Gu, and S.-T. Yau, "Global conformal surface parameterization", In *Proceedings of the Eurographics Symposium on Geometric Processing*, pp.127-137, 2003.

[5] R. Pfeifle and H.-P. Seidel, "Spherical triangular *B*-splines with application to data fitting", *Computer Graphics Forum,* 14(3):89-96, 1995.

[6] H.-P. Seidel, "Polar forms and triangular B-spline surfaces", *Euclidean Geometry and Computers*, pp. 235-286, World Scientific Publishing Co, 1994.

Table 1. Properties of Triangular *B*-splines

	Triangulation	Local control	Convex hull	Affine invariance	Smoothness	Modeling features	Singular points	Applications
Planar spline	Arbitrary	Yes	Yes	Yes	C^{n-1}	Yes	No	Open surfaces, disk-like topology
Spherical spline	Arbitrary	Yes	No	No	C^{n-1}	Yes	No	Sphere-like, genus zero surfaces
Manifold spline	Arbitrary	Yes	Yes	Yes	C^{n-1}	Yes	Yes	Surfaces of complicated topology

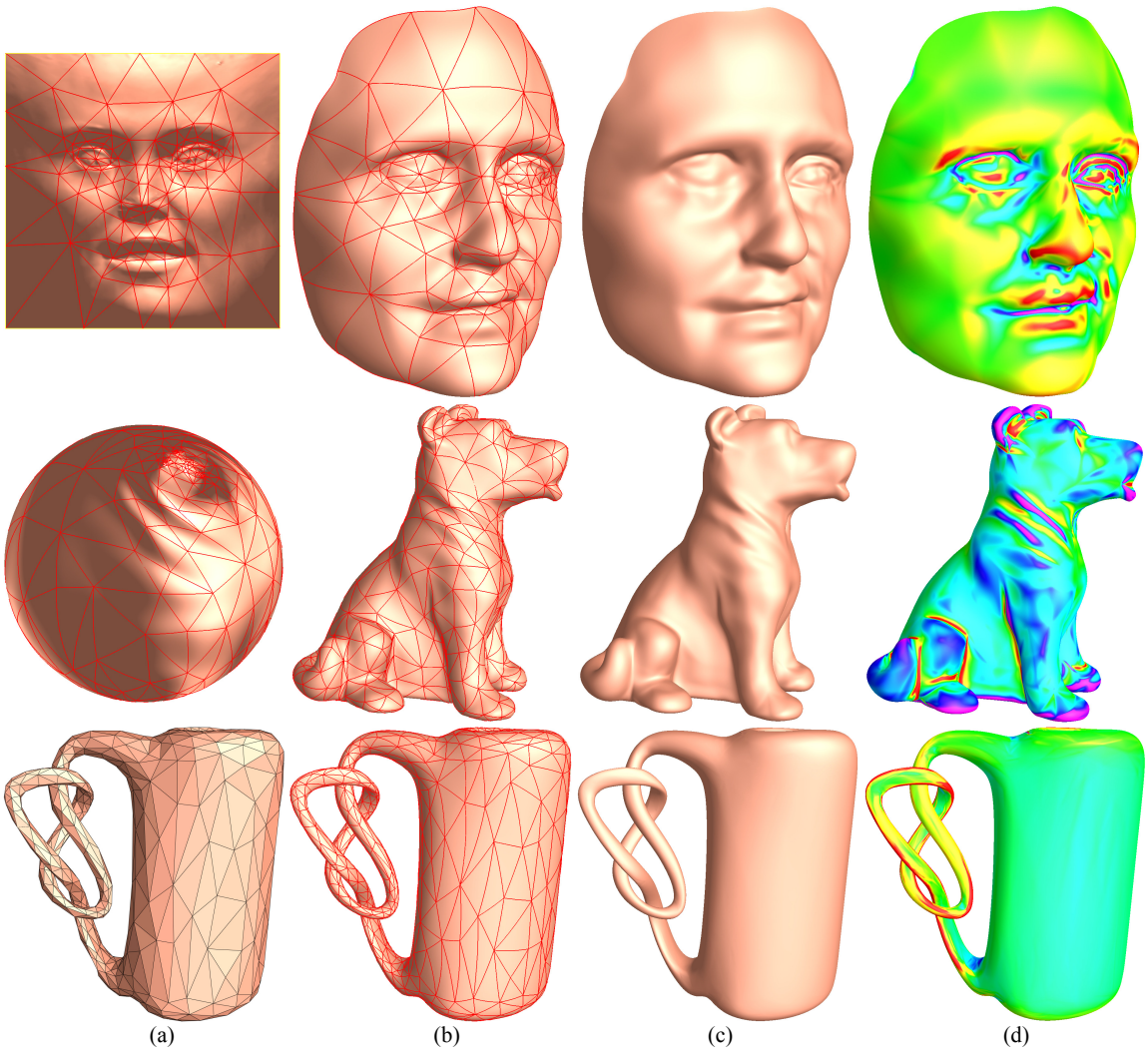

Figure 4. Examples of faired triangular B-splines. Row 1: a C^4 planar spline; Row 2: a C^4 spherical spline; Row 3: a C^2 manifold spline of genus 2 (The other handle is inside the bottle). (a) shows the parametric domain. The red curves on the spline surfaces (b) correspond to the edges in the domain triangulation (a). (c) and (d) show the spline surfaces and mean curvature plot respectively. Note that there is no restriction on the triangulation of the parametric domain. Those knot-lines (curvature concentration on the image of the edges of domain triangulation) are completely eliminated.